2011 American Control Conference
on O'Farrell Street, San Francisco, CA, USA
June 29 - July 01, 2011

Active Braking Control for Two-wheeled Vehicles *via* Switched Second Order Sliding Modes

Mara Tanelli, Antonella Ferrara

Abstract— **The design of an effective braking control system for two-wheeled vehicles is a challenging task, because of the complex dynamic behaviour of the vehicle due to the strong coupling between front and rear wheel and to the dependence of the wheel dynamics on the vehicle speed. To address this problem, this paper proposes to employ a novel switched second order sliding mode (S-SOSM) control strategy grounded on the suboptimal SOSM algorithm, which allows to enhance the closed-loop performance and to tune them to the current working condition.**

I. Introduction and Motivation

Nowadays, four-wheeled vehicles are equipped with many different active control systems which enhance driver and passengers safety, some of which - such as the Anti-lock Braking System (ABS) - have recently become a standard on all cars, see *e.g.*, [1], [2], [3]. In the field of two-wheeled vehicles, instead, such spread of electronic control systems its still in its infancy, as today only a few commercial motorbikes are equipped with ABS systems. Moreover, the few ABS systems available are certified to work only on straight road, see *e.g.*, [4].

In designing active braking control systems for two-wheeled vehicles, it is of utmost importance to be able of devising approaches which offer robustness properties in the face of modeling uncertainties and unknown parameters. In this respect, as the wheel slip dynamics get faster – hence more difficult to control for human drivers – as speed decreases, at low speed reduced tracking performance are acceptable in exchange for increased (and guaranteed) safety. To achieve this, one needs to devise an adaptive control law which adjusts the controller parameters as a function of the vehicle speed, see *e.g.*, [2].

To address this complex control problem, this paper relies on the theory of sliding mode control, which has been shown to be effective in solving the wheel slip control problem both for four- and two-wheeled vehicles, see *e.g.*, [1], [5], [6]. Specifically, a novel switched formulation of second order sliding mode (SOSM) controllers is considered, [6]–[8]. The idea is that of tuning a different SOSM control law for each region of the state space, adapting its parameters to the uncertainty levels and to the possibly different control objectives. More precisely, two different instances of the switched SOSM control algorithm are considered: a full switched SOSM (FS-SOSM), which is tailored to the case in which both the system uncertainties and the control objectives may vary within different regions of the state space, and a gain switched SOSM (GS-SOSM), which allows varying the controller gain in the case of uncertainties with bounds which are constant over the whole state space. The formal investigation of the stability properties of the closed-loop system can be found in [7], [8].

The structure of the paper is as follows. Section II provides a review of the needed notions of SOSM control, while Section III introduces the S-SOSM control approach. Then, Section IV presents the braking control problem for two-wheeled vehicles, whereas in Section V a simulation study assesses the validity of the proposed approach.

II. Preliminaries

For the discussion on the S-SOSM algorithm, it is worth recalling the structure and the basic features of the suboptimal SOSM controller (see *e.g.*, [9]). For simplicity, we consider the so-called *auxiliary* system, which has the form

$$\begin{aligned} \dot{z}_1 &= z_2 \\ \dot{z}_2 &= f(z(t)) + g(z(t))v(t), \end{aligned} \tag{1}$$

where $z_1(t)$ is the sliding variable, $z(t) = [z_1(t)\ z_2(t)]^T \in \mathbb{R}^2$ is the system state, $v(t)$ is the control signal and $f(z(t))$ and $g(z(t))$ are uncertain, sufficiently smooth functions, satisfying all the conditions ensuring existence and uniqueness of the solution [10], together with the following bounds

$$0 < G_1 \leq g(z(t)) \leq G_2, \ \ |f(z(t))| \leq F. \tag{2}$$

The SOSM control problem is formulated as follows: given system (1), where $g(z(t))$ and $f(z(t))$ satisfy (2), design the control signal $v(t)$ so as to steer both $z_1(t)$ and $z_2(t)$ to zero in finite time.

The SOSM controller is such that, under the assumption of being capable of detecting the extremal values z_{Max} of the signal z_1, the following result can be proved.

Theorem 1: (See [9]) Consider system (1), and assume that $g(z(t))$ and $f(z(t))$ satisfy (2). Then, the auxiliary control law

$$\begin{aligned} v(t) &= -\alpha V \ \mathrm{sign}\Big(z_1 - \beta z_{Max}\Big), \quad \beta = \frac{1}{2} \\ \alpha &= \begin{cases} \alpha^* & \text{if} \quad [z_1 - \beta z_{Max}][z_{Max} - z_1] > 0 \\ 1 & \text{else,} \end{cases} \end{aligned} \tag{3}$$

where V is the control gain, α is the so–called modulation factor, and z_{Max} is a piecewise constant function representing the value of the last singular point of $z_1(t)$ (*i.e.*, the most recent value z_{1M} such that $z_2(t_M) = 0$), causes the convergence of the system trajectory onto the sliding

M. Tanelli is with the Dipartimento di Elettronica e Informazione, Politecnico di Milano, Piazza Leonardo da Vinci 32, 20133 Milano, Italy. E-mail: tanelli@elet.polimi.it. A. Ferrara is with the Department of Computer Engineering and Systems Science, University of Pavia, Via Ferrata 1, 27100 Pavia, Italy. E-mail: antonella.ferrara@unipv.it.

manifold $z_1 = z_2 = 0$ in finite time provided that the control parameters α^* and V are chosen so as to satisfy the following constraints

$$\alpha^* \in (0,1] \cap \left(0, \frac{3G_1}{G_2}\right) \tag{4}$$

$$V > \max\left\{\frac{F}{\alpha^* G_1}, \frac{4F}{3G_1 - \alpha^* G_2}\right\}.$$

The control law (3) ensures that the trajectories on the (z_1, z_2) plane are confined within limit parabolic arcs including the origin, and the absolute values of the coordinates of the trajectory intersections with the z_1 and z_2 axis decrease in time. As shown in [9], under conditions (4) one has $|z_1| \leq |z_{Max}|$ and $|z_2| \leq \sqrt{|z_{Max}|}$, and the convergence of $z_{Max}(t)$ to zero takes place in finite time. As a consequence, the origin of the state space is reached in finite time since z_1 and z_2 are both bounded by $\max(|z_{Max}|, \sqrt{|z_{Max}|})$.

For what follows, it is interesting to remark that if one assumes that $f(z(t))$ is a class $\mathcal{K}$ function of z (see *e.g.*, [11]), *i.e.*, the uncertainty is state-dependent, then to achieve global convergence to zero of the system state it is necessary to devise an appropriate initialization phase, which ensures that the first extremal value is reached in finite time. To do this, in [12] it was shown that, assuming that a state-dependent bound of the form

$$|f(z(t))| \leq \overline{F}(z), \tag{5}$$

with $\overline{F}(z)$ being a known $\mathcal{K}$ function of z, holds, then a control law of the type

$$v(t) = -\left(\overline{F}(z) + \kappa^2\right) \operatorname{sign}(z_1(t) - z_1(t_0)), \tag{6}$$

with $\kappa > 0$, globally ensures that the first extremal point is reached in a finite time at $t = t_{M_1}$. Further, for all $t \geq t_{M_1}$, in order to ensure that between two successive extremal points a constant control amplitude can be chosen so that it can counteract the uncertain terms (which do not have *a priori* known constant upper bounds), one needs to employ a control strategy which makes use of a variable commutation point. This means that, instead of using $\beta = \frac{1}{2}$ in (3), a variable value of β is employed. The rationale behind this choice is that the commutation instant (and thus β) is chosen based on the fact that the state norm has exceeded a predefined upper-bound, so as to ensure that the control signal amplitude, tuned according to such a threshold on the uncertainty level, has enough authority to counteract it.

This idea and the approach proposed in [12] will be used in the following for the initialisation phase of the switched control algorithm.

III. The S-SOSM Control Approach

The core idea of the S-SOSM is that of tuning a dedicated SOSM controller for each region of the state space, which is determined by different uncertainty levels and/or by possibly different control objectives. Specifically, we envision two different S-SOSM algorithms: a full switched SOSM (FS-SOSM), and a gain switched SOSM (GS-SOSM). The FS-SOSM allows to tune both the parameters of the SOSM controller, namely α^* and V according to the uncertainty levels of each region. This allows to cope with varying uncertainty and, in parallel, to adapt the controller gain V in view of different requirements associated with each region. On the other hand, the GS-SOSM algorithm has been devised to deal with systems where no different uncertainty levels exist in the different regions of the state space, but the regions are rather associated with different control objectives, *e.g.*, the need of a shorter settling time, of a minimal overshoot, and so on. Thus, in this case it might be possible to achieve these goals by simply adapting the controller gain V, whose minimal value must be chosen so as so satisfy the second of (4).

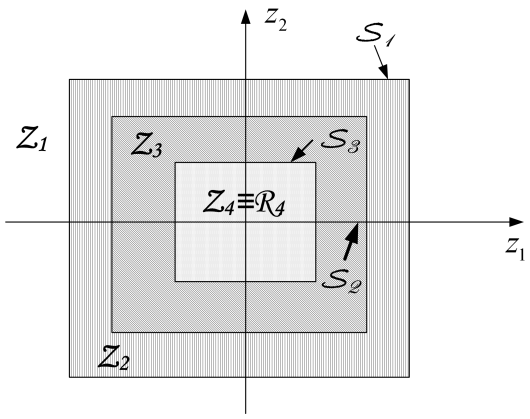

Fig. 1. An example of the state-space partitioning used in the S-SOSM algorithm.

A. Assumptions

To present the S-SOSM control algorithm, for simplicity, we consider again the *auxiliary* system (1). Moreover, we work under the following assumptions.

State-space partitioning

We assume that the state space $\mathcal{Z}$ of system (1) is partitioned in k regions $\mathcal{R}_i$, $i = 1, \cdots, k$, all containing the origin, such that $\cup_i \mathcal{R}_i = \mathcal{Z}$ and with $\mathcal{R}_{i+1} \subset \mathcal{R}_i$. Further, we define as switching surfaces[1] $\mathcal{S}_i = \partial\mathcal{R}_{i+1}$, $i = 1, \cdots, k-1$ (see Figure 1). Finally, we assume that in each region $\mathcal{Z}_i = \mathcal{R}_i \cap \mathcal{R}_{i+1}$, $i = 1, \cdots, k-1$, and in $\mathcal{Z}_k \equiv \mathcal{R}_k$, we may define different upper and lower bounds for the uncertainties, which will be specified in the following. Note that only one of these regions, namely the innermost one $\mathcal{Z}_k$, contains the origin (see again Figure 1). Specifically, in this work it is assumed that the regions $\mathcal{R}_i$, $i = 2, \cdots, k$ are defined as follows

$$\mathcal{R}_i := \{(z_1, z_2) : |z_1| \leq \overline{z}_{1i} \text{ and } |z_2| \leq \overline{z}_{2_i}\}. \tag{7}$$

Uncertainty description

We consider the following bounds on the uncertain terms.

Case 1: Outermost Region $\mathcal{Z}_1$

[1]The boundary of a set M is denoted by ∂M.

In the outermost region $\mathcal{Z}_1$, the following bounds are given

$$\begin{aligned} 0 < G_{11} \leq g(z(t)) \leq G_{21} \\ |f(z(t)| \leq \mathcal{F}_1(z), \end{aligned} \tag{8}$$

where $\mathcal{F}_1(z)$ is a known class $\mathcal{K}$ function of its argument.

Case 2: Regions $\mathcal{Z}_i$, $i = 2, \cdots, k$

In the inner regions $\mathcal{Z}_i$, $i = 2, \cdots, k$, the uncertainties are described as

$$\begin{aligned} 0 < \mathcal{G}_{1i}(z) \leq g(z(t)) \leq \mathcal{G}_{2i}(z) \\ |f(z(t)| \leq \mathcal{F}_i(z), \end{aligned} \tag{9}$$

where

$$\begin{aligned} \mathcal{G}_{ji}(z) = G_{ji}(z) + \overline{G}_{ji},\ j = \{1, 2\} \\ \mathcal{F}_i(z) = F_i(z), \end{aligned} \tag{10}$$

where $G_{1i}(\cdot)$, $G_{2i}(\cdot)$ and $F_i(\cdot)$ are known class $\mathcal{K}$ functions and $\overline{G}_{1i}$, $\overline{G}_{2i}$ are known positive constants. Further, as in the inner regions it is possible to bound the state of the system (recall that (7) implies that the region boundaries are given for $\mathcal{Z}_i$, $i = 2, \cdots, k$), a constant upper bound on the uncertain terms is assumed to be known, *i.e.*, $\forall\, i = 2, \cdots, k$, we can write

$$\begin{aligned} 0 < \overline{\mathcal{G}}_{1i} \leq g(z(t)) \leq \overline{\mathcal{G}}_{2i} \\ |f(z(t))| \leq \overline{\mathcal{F}}_i. \end{aligned} \tag{11}$$

Finally, note that to detect which is the currently active region of the state space, one in principle needs a measure of both the sliding variable z_1 and its first derivative z_2. This is not a significant limitation for the proposed control strategies, as to compute z_2 it suffices to employ a Levant differentiator thereby asking for a measurement of the sliding variable only. In the following, we will formulate the S-SOSM algorithms making use of the first-order Levant differentiator, [13].

B. The S-SOSM Control Algorithms

We are now ready to introduce the switched SOSM algorithms.

Algorithm 3.1: (FS-SOSM)

Consider system (1), with the state space partitioned as discussed above. Assume that a measurement of $z_1(t)$ is given, and compute the estimate of z_2, denoted by $\hat{z}_2$ as:

$$\begin{aligned} \dot{\zeta} = \hat{z}_2, \quad \hat{z}_2 = -\gamma_0 |\zeta - z_1|^{1/2} \text{sign}(\zeta - \text{z}_1) + \nu_1 \\ \dot{\nu}_1 = -\gamma_1 \text{sign}(\zeta - \text{z}_1), \end{aligned} \tag{12}$$

where γ_0 and γ_1 are positive constants chosen on the basis of a known bound on the Lipschitz constant of the derivative of z_1, [13].

Assume also that, for $z \in \mathcal{Z}_1$, $g(z(t))$ and $f(z(t))$ satisfy constraints (8), whereas for each $z \in \mathcal{Z}_i$, $i = 2, \cdots, k$, $g(z(t))$ and $f(z(t))$ satisfy constraints (11).

If $z \in \mathcal{Z}_1$, over the time interval to the first extremal point, *i.e.*, for $0 \leq t \leq t_{M_1}$, define the control signal as

$$\begin{aligned} v(t) = -\frac{1}{G_{11}} \big[\mathcal{F}_1(z(t)) + \nu\big] \text{sign}\,(z_1(0)),\ t = 0 \\ v(t) = -\frac{1}{G_{11}} \big[\mathcal{F}_1(z(t)) + \nu\big] \text{sign}\,(z_1(t) - z_1(0)),\ 0 < t \leq t_{M_1} \end{aligned} \tag{13}$$

with $\nu > 0$. Then, over the time interval $t_{M_j} \leq t \leq t_{M_{j+1}}$ such that $z(t) \in \mathcal{Z}_1$, adopt the control law

$$v(t) = -V_{M_j}\ \text{sign}\Big(z_1(t) - \beta_j z_{1_{M_j}}\Big), \tag{14}$$

with

$$\begin{aligned} V_{M_j} = \frac{\pi}{G_{11}} \left[\overline{\mathcal{F}}_1 + \frac{1}{3}\eta^2\right], \quad \pi > 1 \\ \beta_j = \max\left\{\frac{1}{2}, 1 - \frac{\eta^2}{2\left[\overline{\mathcal{F}}_1 + G_{21} V_{M_j}\right]}\right\}, \end{aligned} \tag{15}$$

where η is a positive constant, $\overline{\mathcal{F}}_1 = \overline{\mathcal{F}}_1(|z_1(t_{M_j})|, \eta\sqrt{|z_1(t_{M_j})|})$ is an upper bound on the function $\mathcal{F}_1(z)$ computed at any time instant $\{t_{M_j}\}$, and the sequence $\{t_{M_j}\}$ is made up of the time instants at which $z_2 = 0$ and $z_{1_{M_j}} = z_1(t_{M_j})$ (see [12]).

If $z \in \mathcal{Z}_i$, $i = 2, \cdots, k$, define the control signal as

$$\begin{aligned} v(t) = -\alpha_i V_i\ \text{sign}\Big(z_1 - \frac{1}{2} z_{Max}\Big) \\ \alpha_i = \begin{cases} \alpha_i^* & \text{if} \quad [z_1 - \frac{1}{2} z_{Max}][z_{Max} - z_1] > 0 \\ 1 & \text{else,} \end{cases} \end{aligned} \tag{16}$$

where V_i is the control gain for the i-th region, α_i is the $i-$th modulation factor, and all the other quantities have the same meaning as in Theorem 1. The control parameters α_i^* and V_i are chosen so as to satisfy the following constraints

$$\begin{aligned} \alpha_i^* \in (0, 1] \cap \left(0, \frac{3\overline{\mathcal{G}}_{1i}}{\overline{\mathcal{G}}_{2i}}\right) \\ V_i > \max\left\{\frac{\overline{\mathcal{F}}_i}{\alpha_i^* \overline{\mathcal{G}}_{1i}}, \frac{4\overline{\mathcal{F}}_i}{3\overline{\mathcal{G}}_{1i} - \alpha_i^* \overline{\mathcal{G}}_{2i}}\right\} \\ V_i > V_{Max} = \max_{i=2,\ldots,k}\left\{\frac{\overline{\mathcal{F}}_i}{\alpha_i^* \overline{\mathcal{G}}_{1i}}\right\}. \end{aligned} \tag{17}$$

Algorithm 3.2: (GS-SOSM)

The GS-SOSM algorithm is analogous to the FS-SOSM one, with the only difference that we assume that the bounds on the uncertain functions $g(z(t))$ and $f(z(t))$ are as in (2), *i.e.*, constant over all state space regions $\mathcal{Z}_i$. In this case, if $z \in \mathcal{Z}_i$, the control signal is defined as

$$\begin{aligned} v(t) = -\alpha V_i\ \text{sign}\Big(z_1 - \frac{1}{2} z_{Max}\Big) \\ \alpha = \begin{cases} \alpha^* & \text{if} \quad [z_1 - \frac{1}{2} z_{Max}][z_{Max} - z_1] > 0 \\ 1 & \text{else,} \end{cases} \end{aligned} \tag{18}$$

where V_i is the control gain for the i-th region, α is the constant modulation factor and all the other quantities have the same meaning as in Theorem 1. The control parameters α^* and V_i are chosen so as to satisfy the following constraints

$$\begin{aligned} \alpha^* \in (0, 1] \cap \left(0, \frac{3G_1}{G_2}\right) \\ V_i > \overline{V} = \max\left\{\frac{F}{\alpha^* G_1}, \frac{4F}{3G_1 - \alpha^* G_2}\right\}. \end{aligned} \tag{19}$$

Remark 3.1: In practice, one may expect that it would be more natural to define the state space partitioning based on

which different control specifications and/or different levels of uncertainties are defined directly in the state space of the original system rather than in that of the auxiliary one. How to map regions defined in the former system into regions of the latter one is an open problem, and topic of ongoing research.

IV. The Braking Control Problem in Two-Wheeled Vehicles

This section presents the SOSM approach to the active braking control problem for two-wheeled vehicles. To this end, we first introduce the dynamical model and then show how to design both a traditional SOSM controller and the proposed switched ones. Motivated by the fact that we consider braking maneuvers taking place on a straight line, the two-wheeled vehicle dynamics can be expressed as

$$\begin{cases} J\dot{\omega}_f = r_f F_{x_f} - T_{b_f} \\ J\dot{\omega}_r = r_r F_{x_r} - T_{b_r} \\ m\dot{v} = -F_{x_f} - F_{x_r}, \end{cases} \tag{20}$$

where ω_f and ω_r [rad/s] are the angular speed of the front and rear wheels, respectively, $v\,[m/s]$ is the longitudinal speed of the vehicle center of mass, T_{b_f} and T_{b_r} [Nm] are the front and rear braking torques, F_{x_f} and F_{x_r} [N] are the front and rear longitudinal tire-road contact forces, $J\,[kg\,m^2]$, $m\,[kg]$ and $r_f = r_r = r\,[m]$ are the moment of inertia of the wheel, the vehicle mass, and the wheel radii, respectively. The system is nonlinear due to the dependence of F_{x_i}, $i = \{f, r\}$, on the state variables v and ω_i, $i = \{f, r\}$. The expression of F_{x_i} can be well-approximated as follows, [3]

$$F_{x_i} = F_{z_i}\,\mu(\lambda_i, a_{i_t}; \vartheta), \quad i = \{f, r\}, \tag{21}$$

where F_{z_i} is the vertical force at the tire-road contact point and $\mu(\cdot, \cdot; \vartheta)$ is a function of: (i) the longitudinal slip $\lambda_i \in [0, 1]$, which, during braking, is defined as $\lambda_i = \big(v - \omega_i r\big)/v$; (ii) the wheel side-slip angle a_{i_t}. Vector ϑ in $\mu(\cdot, \cdot; \vartheta)$ represents the set of parameters that identify the tire-road friction condition. Since for braking maneuvers performed along a straight line one can set the wheel side-slip angle equal to zero ($a_{i_t} = 0$), we shall omit the dependence of F_{x_i} on a_{i_t} and denote the μ function as $\mu(\cdot; \vartheta)$. Note, in passing, that from (21) one has that the longitudinal force produced by a wheel is bounded, *i.e.*,

$$|F_{xi}| \leq \Psi, \qquad i \in \{f, r\}. \tag{22}$$

The tire model (21) is a steady-state model of the interaction between the tire and the road. The transient tire behavior, due to tire relaxation dynamics, yields traction forces F_{xi} with bounded first time derivative, *i.e.*,

$$|\dot{F}_{xi}| \leq \Gamma, \qquad i \in \{f, r\}. \tag{23}$$

Many empirical analytical expressions for function $\mu(\cdot; \vartheta)$ have been proposed in the literature. A widely-used expression (see *e.g.*, [3]) is

$$\mu(\lambda; \vartheta) = \vartheta_1(1 - e^{-\lambda\vartheta_2}) - \lambda\vartheta_3, \tag{24}$$

where ϑ_i, $i = 1, 2, 3$, are the three components of vector ϑ. By changing the values of these three parameters, many different tire-road friction conditions can be modeled. In Figure 2(a) the shape of $\mu(\lambda; \vartheta)$ in four different conditions is displayed. From now on, for ease of notation, the dependency of μ on ϑ will be omitted, and the function in equation (24) will be referred to as $\mu(\lambda)$.

To complete the description of F_{x_i} in (21), we just have to specify the expression for F_{z_i}. To describe the load transfer phenomena between front and rear axles, we model the vertical force on the front and rear wheels as follows

$$\begin{aligned} F_{z_f} &= \frac{mgl_r}{l} - \frac{mh}{l}\dot{v} = W_f - \Delta_{F_z}\dot{v} \\ F_{z_r} &= \frac{mgl_f}{l} + \frac{mh}{l}\dot{v} = W_r + \Delta_{F_z}\dot{v}, \end{aligned} \tag{25}$$

where l is the wheelbase, l_f and l_r are the distances between the projection of the center of mass on the road and the front and rear wheel contact points, respectively, h is the height of the center of mass and g is the gravitational acceleration. Note that $\dot{v}$ is the vehicle acceleration, hence it is negative during braking.

In system (20) the state variables are v and ω_i. As λ_i, v and ω_i are linked by the algebraic equation given by the definition of the wheel slip itself, it is possible to replace ω_i with λ_i as state variable. This, using expressions (21) and (25) leads to the system

$$\begin{cases} \dot{\lambda}_f = -\frac{r}{Jv}\left(\Psi_f(\lambda_f, \lambda_r) - T_{b_f}\right) \\ \dot{\lambda}_r = -\frac{r}{Jv}\left(\Psi_r(\lambda_f, \lambda_r) - T_{b_r}\right) \\ \dot{v} = -\frac{W_f\mu(\lambda_f) + W_r\mu(\lambda_r)}{m - \Delta_{F_z}(\mu(\lambda_f) - \mu(\lambda_r))}, \end{cases} \tag{26}$$

where

$$\Psi_f(\lambda_f, \lambda_r) = \left[r(W_f - \Delta_{F_z}\dot{v})\mu(\lambda_f) - \frac{J}{r}(1 - \lambda_f)\dot{v}\right] \tag{27}$$

$$\Psi_r(\lambda_f, \lambda_r) = \left[r(W_r + \Delta_{F_z}\dot{v})\mu(\lambda_r) - \frac{J}{r}(1 - \lambda_r)\dot{v}\right]. \tag{28}$$

Figures 2(b) and 2(c) show a plot of the functions $\Psi_f(\cdot, \lambda_r)$ and $\Psi_r(\lambda_f, \cdot)$, respectively, obtained for different values of λ_r and λ_f. As it is apparent by inspecting these figures, the front wheel behavior is substantially independent from that of the rear wheel, while the latter is strongly coupled to the front one. This can be explained noticing that $\Psi_f(\cdot, \lambda_r)$ and $\Psi_r(\lambda_f, \cdot)$ are different in magnitude, as the term $\Delta_{F_z}\dot{v}$ changes sign. This makes $\Psi_r(\lambda_f, \cdot)$ much more sensitive to the variations in the front wheel slip λ_f. In what follows we disregard the dependence of $\Psi_f(\lambda_f, \lambda_r)$ on λ_r and adopt the notation $\Psi_f(\lambda_f)$.

It is worth noting that the dependence of $\Psi_r(\lambda_f, \cdot)$ on λ_f can be easily dealt with with a SM approach, as the function $\Psi_r(\lambda_f, \cdot)$ is in any case bounded, and a worst-case approach can be pursued so as to account for the variability of the tyre–road friction model with the front wheel slip. This makes the proposed approach particularly attractive for the problem at hand, as it allows us to design two single-input-single-output (SISO) wheel slip controllers, one for each wheel, where the coupling only affects the definition of the bounds on the uncertain terms.

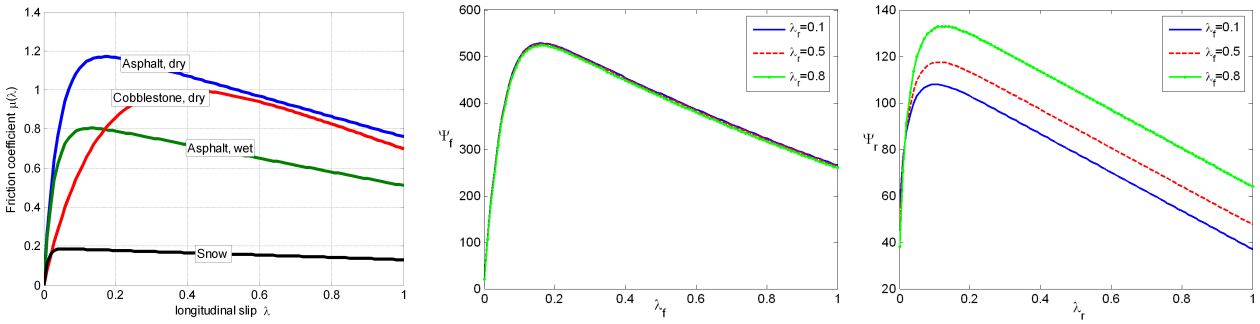

(a) (b) (c)

Fig. 2. Plot of: (a) the function $\mu(\lambda;\vartheta)$ in different road conditions; (b) $\Psi_f(\cdot,\lambda_r)$ for different values of λ_r: $\lambda_r = 0.1$ (solid line), $\lambda_r = 0.5$ (dashed line) and $\lambda_r = 0.1$ (dotted line); (c) $\Psi_r(\lambda_f,\cdot)$ for different values of λ_f: $\lambda_f = 0.1$ (solid line), $\lambda_f = 0.5$ (dashed line) and $\lambda_f = 0.1$ (dotted line).

A. S-SOSM Traction Controller Design

Based on the above discussion, two SISO SOSM controllers will be designed based on the wheel slip dynamics λ_i, $i = \{f, r\}$, disregarding at this stage the actuator dynamics. This allows to work on a plant with relative degree one, and to carry out the control design based on standard SOSM theory with chattering alleviation, [9]. The effect of the actuator dynamics will be taken into account in the simulations carried out in Section V. Thus, the braking controller is designed to steer the wheel slips λ_i, $i = \{f, r\}$ to the desired value λ_i^*. The error between the current slip and the desired slip is chosen as the sliding variable, *i.e.*,

$$s_i = \lambda_i - \lambda_i^*, \quad i = \{f, r\} \tag{29}$$

and the control objective is to design a continuous control law $\mathcal{T}_i$ capable of steering this error to zero in finite time. Then, the chosen sliding manifold is given by $s_i = 0$.

The first and second time derivatives of the sliding variable s_i are

$$\begin{cases} \dot{s}_i &= \dot{\lambda}_i - \dot{\lambda}_i^* \\ \ddot{s}_i &= \varphi_i + h_i \dot{\mathcal{T}}_i, \end{cases} \tag{30}$$

where $\dot{\lambda}_i$ is given by the first and the second of (26), and h_i and φ_i are defined as

$$h_i := \frac{r}{Jv} \tag{31}$$

$$\varphi_i := \frac{r\omega_i}{v^2}\ddot{v} + 2\frac{r\dot{\omega}_i\dot{v}}{v^2} - 2\frac{r\omega_i\dot{v}^2}{v^3} - \frac{r^2}{Jv}\dot{F}_{xi} - \ddot{\lambda}_i^*. \tag{32}$$

Combining the third of (20) with (22), it yields

$$|\dot{v}| \leq \frac{2\Psi}{m} = f_1. \tag{33}$$

Further, taking into account the first time derivative of the third of (20), (23), and (33), one has that

$$|\ddot{v}| \leq \frac{2\Gamma}{m} = f_2. \tag{34}$$

Finally, from the first and second of (20) and (22), one gets

$$|\dot{\omega}_i| \leq \frac{r\Psi - T_{bi}}{J} = f_3(T_{bi}). \tag{35}$$

Relying on (33), (34), and (35), and assuming $v > 0$, $\omega_i > 0$, hence $\lambda_i \in [0, 1)$ one has that φ_i is bounded. From a physical viewpoint, this means that, when a constant driving torque T is applied, the second time derivative of the rear wheel slip is bounded.

Note that, to design a SOSM controller, we only need to assume that suitable bounds of φ_i, $i = \{f, r\}$, are known, *i.e.*, $|\varphi_i| \leq \Phi_i(v, \omega_i, T_{bi})$. Similar considerations can be made for h_i, $i = \{f, r\}$, which can be regarded as unknown bounded functions with the following known bounds $0 < \Gamma_{i1}(v, \omega_i) \leq h_i \leq \Gamma_{i2}(v, \omega_i)$.

Remark 4.1: It is worth noting that the uncertain functions h_i and φ_i in (31) and (32) are functions of the vehicle speed. Further, in view of the wheel slip definition and considering that the chosen sliding variable is the slip tracking error (see Equation (29)), designing an S-SOSM controller considering the vehicle speed v as switching variable means that the switching regions will be defined based on the speed and the deceleration. This allows accounting for a safety objective, ensured by adapting the braking performance to the vehicle speed, and to a comfort objective, taken into account by considering different levels of deceleration. This highlights the flexibility of the proposed approach, which offers the possibility of incorporating into the design different performance objectives.

V. Simulation Results

This section is devoted to analyse the performance of the proposed S-SOSM controllers via a simulation study, carried out with a detailed dynamical model of a two-wheeled vehicle, in which the suspensions dynamics are explicitly modeled, and tire elasticity and tire relaxation dynamics [14] are also taken into account. As for the actuator, a first order low-pass filter with a bandwidth of 10 Hz has been employed. For comparison purposes, we will consider a standard SOSM controller, which has constant and fixed parameters α^* and V. Then, to demonstrate that by adapting the controller parameters to the vehicle speed a faster transient can be achieved at low speed, when controlling the motorcycle is more critical, while privileging the tracking objective at higher speeds, a GS-SOSM and a FS-SOSM controller have been designed, considering as switching parameter the vehicle speed and mapping it onto the sliding variables in (30).

To compare the performance of the three considered controllers, a wheel slip set point has been defined which is a sequence of steps (each with width 0.05) from 0 to 0.2, thus testing the closed-loop system capability of tracking also wheel slip values beyond the peak of the tire-road friction curve (see Figure 2(a)), and it is carried out on dry road. Four switching thresholds have been defined; thus, we have one controller setting for $v \leq 10\,\text{m/s}$, a second one for $10 < v \leq 18\,\text{m/s}$, a third for $18 < v \leq 25\,\text{m/s}$, and the last one (which is equal to that used for the fixed structure SOSM controller) for speed values above 25 m/s. Note that the base value for the controller gain V has been tuned differently for the front and for the rear wheel controller, so as to take into account the difference in the load distribution and ensure a similar transient performance at the two wheels.

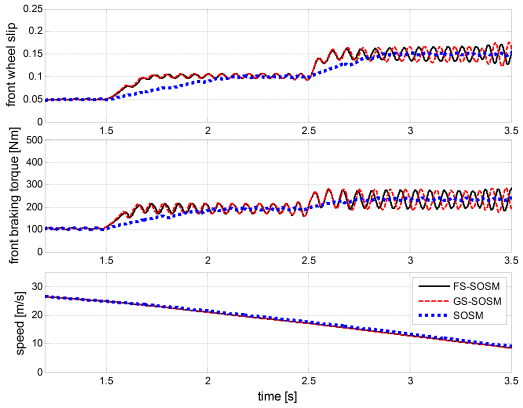

Fig. 3. Detail of a braking maneuver where the front slip set-point is varied stepwise from $\lambda_f^* = 0.05$ to $\lambda_f^* = 0.15$. Traditional SOSM controller (dotted line), GS-SOSM (dashed line) and FS-SOSM (solid line). Time histories of the front wheel slip (top), of the front braking torque (middle) and of the vehicle speed (bottom).

Figure 3 shows the time histories of the closed-loop front wheel slip, braking torque and vehicle speed in the considered braking maneuver; specifically, a detail of the second and third step variation is shown. By inspecting this figure, note that the wheel slip exhibits small oscillations; as was observed in [5], such oscillations are due to the fact that the presence of the unmodelled actuator dynamic increases the relative degree of the system. Coherently with the results in [5], the amplitude of such oscillations increases with the controller gain, and it is thus more significant when the switched algorithms are used, especially as the vehicle speed decreases and hence a large gain value is used. However, from a practical purpose, such oscillations can be well tolerated in the specific application. Similar results have been obtained for the rear wheel slip.

Finally, to quantitatively evaluate the performance gain achieved with the proposed switched controllers, we consider as a cost function the Root Mean Square Error (RMSE) of the tracking error, represented by the sliding variable s, *i.e.*, $J_s = \sqrt{\sum_{i=1}^{N} s(i)^2/N}$, where N is the number of samples in the simulation run. Specifically, to better compare the control algorithms we computed a normalized version the

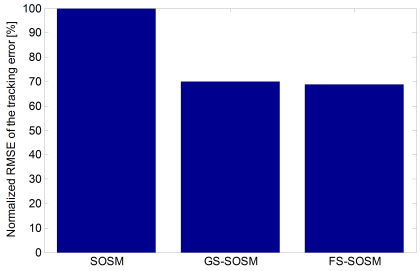

Fig. 4. Percentage value of the normalized RMSE of the tracking error with the three controllers.

cost function, defined as

$$J_{s_{Norm}} = 100 \frac{J_s}{\max_{i=1,\ldots,3}\{J_{s_i}\}}, \quad [\%], \tag{36}$$

which represents, in percent, the tracking error normalized with respect to the worst case among the three considered controllers. Figure 4 shows the values of (36) obtained in the considered braking maneuver. As can be seen, the switched algorithms allow for a 30% improvement with respect to the standard SOSM one.

REFERENCES

[1] S. Drakunov, U. Özgüner, P. Dix, and B. Ashrafi, "ABS control using optimum search via sliding modes," *IEEE Transactions on Control Systems Technology*, vol. 3, no. 1, pp. 79–85, 1995.

[2] T. Johansen, I. Petersen, J. Kalkkuhl, and J. Lüdemann, "Gain-scheduled wheel slip control in automotive brake systems," *IEEE Transactions on Control Systems Technology*, vol. 11, no. 6, pp. 799–811, November 2003.

[3] S. Savaresi and M. Tanelli, *Active Braking Control Systems Design for Vehicles*. London, UK: Springer-Verlag, 2010.

[4] M. Corno, S. Savaresi, M. Tanelli, and L. Fabbri, "On optimal motorcycle braking." *Control Engineering Practice*, vol. 16, no. 6, pp. 644–657, 2008.

[5] M. Tanelli, C. Vecchio, M. Corno, A. Ferrara, and S. Savaresi, "Traction control for ride-by-wire sport motorcycles: a second order sliding mode approach," *IEEE Transactions on Industrial Electronics*, vol. 56, no. 9, pp. 3347–3356, 2009.

[6] M. Tanelli, A. Ferrara, and C. Vecchio, "Switched second order sliding mode for wheel slip control of road vehicles," in *Proceedings of the IEEE Variable Structure Systems Conference, VSS 2010*, Mexico City, Mexico, 2010.

[7] M. Tanelli and A. Ferrara, "Switched second order sliding mode control," in *Proceedings of the IEEE Conference on Decision and Control, CDC 2010*, Atlanta, GA, 2010.

[8] ——, "Switched second order sliding mode control," Politecnico di Milano, Tech. Rep., 2010.

[9] G. Bartolini, A. Ferrara, and E. Usai, "Chattering avoidance by second-order sliding mode control," *IEEE Transactions on Automatic Control*, vol. 43, no. 2, pp. 241–246, 1998.

[10] H. Khalil, *Nonlinear Systems*. Upper Saddle River, New Jersey: 2nd Edition, Prentice Hall, 1996.

[11] A. Isidori, *Nonlinear Control Systems*. London: 3rd Edition, Spriger, 1995.

[12] G. Bartolini, A. Pisano, and E. Usai, "Global Stabilization for Nonlinear Uncertain Systems with Unmodeled Actuator Dynamics," *IEEE Transactions on Automatic Control*, vol. 46, no. 11, pp. 1826–1832, 2001.

[13] A. Levant, "Robust exact differentiation via sliding mode technique," *Automatica*, vol. 34, no. 3, pp. 379–384, 1998.

[14] U. Kiencke and L. Nielsen, *Automotive Control Systems*. Springer-Verlag, Berlin, 2000.